Valence-Dependent Metal−Metal Bonding and Optical Spectra in Confacial Bioctahedral $[Re_2Cl_9]^{z-}$ ($z = 1, 2, 3$). Crystallographic and Computational Characterization of $[Re_2Cl_9]^-$ and $[Re_2Cl_9]^{2-}$

Graham A. Heath,* John E. McGrady, Raphael G. Raptis, and Anthony C. Willis

The Research School of Chemistry, The Australian National University, Canberra, ACT 0200, Australia

Received December 15, 1995[⊗]

The geometric structure of the confacial bioctahedral $[Re_2Cl_9]^{z-}$ anion has been determined by single-crystal X-ray diffraction in two distinct oxidation states, Re^{IV}_2 and $Re^{III}Re^{IV}$. $[Bu_4N][Re_2Cl_9]$ crystallizes in the monoclinic space group $P2_1/m$ [a/Å = 10.6363(3), b/Å = 11.420(1), c/Å = 13.612(1), β/deg = 111.18(1), $Z = 2$], while $[Et_4N]_2[Re_2Cl_9]$ crystallizes in the orthorhombic space group *Pnma* [a/Å = 15.82(1), b/Å = 8.55(2), c/Å = 22.52(3), $Z = 4$]. The Re−Re separation contracts from 2.704(1) Å in $[Bu_4N][Re_2Cl_9]$ to 2.473(4) Å in $[Et_4N]_2[Re_2Cl_9]$ (or, equivalently, from 2.725 to 2.481 Å after standard corrections for thermal motions), while the formal metal−metal bond order *falls* from 3.0 to 2.5. SCF−Xα−SW molecular orbital calculations show that, despite the $\{d^3d^3\}$ configuration, the single σ bond in $[Re_2Cl_9]^-$ dominates the observed structural properties. For $[Re_2Cl_9]^{2-}$, the 0.23 Å contraction in Re−Re is attributed jointly to radial expansion of the Re 5d orbitals and to diminished metal−metal electrostatic repulsion, which act in concert to make both σ and δ_π bonding more important in the reduced species. Computed transition energies and oscillator strengths for the two structurally defined anions permit rational analysis of their ultraviolet spectra, which involve both $\sigma \rightarrow \sigma^*$ and halide-to-metal charge-transfer absorptions. The intense $\sigma \rightarrow \sigma^*$ band progresses from 31 000 cm^{-1} in $[Re_2Cl_9]^-$ to 36 400 cm^{-1} in $[Re_2Cl_9]^{2-}$, according to the present assignments. For electrogenerated, highly reactive $[Re_2Cl_9]^{3-}$ (where conventional X-ray structural information is unlikely to become available), the dominant absorption band advances to 40 000 cm^{-1}, suggesting further strengthening of the metal−metal σ bond in the Re^{III}_2 species.

Introduction

The confacial bioctahedral structure holds a central position in transition metal halide chemistry, and the extensive array of well-characterized M_2X_9 complexes provides an unrivaled opportunity to study periodic progressions in metal−metal bonding within an isostructural family.[1,2] The vertical trend is generally exemplified by the $\{d^3d^3\}$ nonachlorides of the Cr, Mo, W triad, where binuclear magnetic coupling is greatest for the third-row element. A recent direct comparison of $\{d^5d^5\}$ $[Ru_2Br_9]^{3-}$ and $[Os_2Br_9]^{3-}$ likewise demonstrates considerably stronger interaction in the complex of the heavier metal, and in this instructive case the net metal−metal bonding is necessarily purely σ in nature.[3] In addition, the redox chemistry of the transition-metal nonahalides in solution is now well established and has added substantially to appreciation of horizontal and vertical periodic relationships in their electronic structure and bonding. Through *in situ* electrogeneration, the optical spectra of $[Ru_2X_9]^{z-}$ ($z = 1-4$; X = Cl, Br),[4] $[Os_2Br_9]^{z-}$ ($z = 1-3$),[5] and $[Re_2Cl_9]^{z-}$ ($z = 1-3$)[6] are known in some detail, and those of $[W_2Cl_9]^{z-}$, $[Tc_2Br_9]^{z-}$, $[Os_2Cl_9]^{z-}$, and $[Ir_2Cl_9]^{z-}$ ($z = 1-3$) have recently been measured in our laboratory. However, *crystallographic* characterization of a given binuclear nonahalide in two distinct oxidation states is much more elusive. The only reported example is provided by the valence pair $[W_2Cl_9]^{2-}$ and $[W_2Cl_9]^{3-}$, where the metal−metal separation contracts (by 0.13 Å) as the δ_π bonding level is filled.[7,8]

Preliminary structural analysis of neighboring $[^nBu_4N][Re_2Cl_9]$ was undertaken as early as 1969,[9] but difficulties arose, and only the approximate Re−Re distance and other critical dimensions have been cited elsewhere.[10] The stepwise, reversible $[Re_2Cl_9]^{1-/2-}$ and $[Re_2Cl_9]^{2-/3-}$ electrode potentials fall at +0.75 and −0.17 V, respectively, *vs* Ag/AgCl.[6] This means that the Re^{IV}_2 starting complex is readily reduced, and we now describe the complete crystallographic characterization of both members of the $[Re_2Cl_9]^{1-/2-}$ couple. In contrast to the ditungsten system mentioned above, one-electron reduction to form $Re^{III}Re^{IV}$ involves population of the antibonding (δ_π*) level. Despite this, a further substantial contraction of the metal−metal separation (by 0.23 Å) is revealed.

The ultraviolet and visible spectra of early transition-metal MX_6 and M_2X_9 complexes are rich in intense halide-to-metal charge-transfer bands.[11] However, for binuclear systems there is abiding interest in the possibility of identifying the $\sigma \rightarrow \sigma^*$ transition as an index of bonding within the MX_3M core. Furnished with the requisite geometric information for both $[Re_2Cl_9]^-$ and $[Re_2Cl_9]^{2-}$, we have computed the ground-state electronic structures (by SCF−Xα−SW methods) and gone on to calculate the anticipated electronic transition energies and oscillator strengths for each oxidation state.[2] On this basis, cogent assignments of the observed optical spectra (from 5000 to 50 000 cm^{-1}) can be made for structurally characterized

[⊗] Abstract published in *Advance ACS Abstracts,* May 15, 1996.

(1) Cotton, F. A.; Walton, R. A. *Multiple Bonds between Metal Atoms*; Oxford University Press: Oxford, England, 1993.
(2) McGrady, J. E. Ph.D. Thesis, The Australian National University, 1994.
(3) Gheller, S. F.; Heath, G. A.; Hockless, D. C. R.; Humphrey, D. G.; McGrady, J. E. *Inorg. Chem.* **1994**, *33*, 3986.
(4) Kennedy, B. J.; Heath, G. A.; Khoo, T. J. *Inorg. Chim. Acta* **1991**, *190*, 265.
(5) Heath, G. A.; Humphrey, D. G. *J. Chem. Soc., Chem. Commun.* **1990**, 672.
(6) Heath, G. A.; Raptis, R. G. *Inorg. Chem.* **1991**, *30*, 4106.
(7) Watson, W. H., Jr.; Waser, J. *Acta Crystallogr.* **1958**, *11*, 689.
(8) Cotton, F. A.; Falvello, L. R.; Mott, G. N.; Schrock, R. R.; Sturgeoff, L. G. *Inorg. Chem.* **1983**, *22*, 2621.
(9) Stokeley, P. F. Ph.D. Thesis, Massechusetts Institute of Technology, 1969.
(10) Cotton, F. A.; Ucko, D. A. *Inorg. Chim. Acta* **1972**, *6*, 161.
(11) Heath, G. A.; McGrady, J. E. *J. Chem. Soc., Dalton Trans.* **1994**, 3767.

S0020-1669(95)01604-1 CCC: $12.00

Table 1. Crystallographic Data for $[Bu_4N][Re_2Cl_9]$ (**I**) and $[Et_4N]_2[Re_2Cl_9]$ (**II**)

	I	**II**
fw	933.96	952.00
space group	$P2_{1/m}$	Pnma
a/Å	10.636(3)	15.82(1)
b/Å	11.420(1)	8.55(2)
c/Å	13.612(1)	22.52(3)
β/deg	111.18(1)	{90}
V/Å^3	1541.6(4)	3047(9)
T/deg	20(1)	26(1)
λ/Å	1.5418	1.5418
Z	2	4
ρ_{calcd}/(g cm^{-3})	2.012	2.075
abs coeff, μ/cm^{-1}	22.06	22.13
R[a]	0.046	0.065
R_w[b]	0.061	0.090

[a] $R = \sum(|F_o| - |F_c|)/\sum|F_o|$ and $R_w = [\sum w(|F_o| - |F_c|)^2/\sum(w|F_o|^2)]^{1/2}$.

$\{d^3d^3\}$ $[Re_2Cl_9]^-$ and $\{d^3d^4\}$ $[Re_2Cl_9]^{2-}$. The trends that emerge make it possible to assign the solution spectrum of electrogenerated $[Re_2Cl_9]^{3-}$ as well and to draw interesting conclusions about the molecular structure of this highly reactive$\{d^4d^4\}$ species.

Experimental Methods

The di-tetravalent complex, $[^nBu_4N][Re_2Cl_9]$ (**I**), was prepared by the literature procedure,[12] and found to separate as deep green-brown crystals from CH_2Cl_2. Mixed-valence $[Et_4N]_2[Re_2Cl_9]$ (**II**) was isolated by gently stirring the green solution of $[^nBu_4N][Re_2Cl_9]$ in CH_2Cl_2 with an excess of Et_4NCl until spontaneous reduction was complete and dark purple crystals separated (typically 3−5 min, monitored spectroscopically). Lattice parameters for **I** and **II** were determined by least-squares analysis of the setting angles of high-angle reflections. Intensity data were collected for quartz-fiber mounted crystals by $\omega-2\theta$ scans with graphite-monochromated Cu-Kα_1 radiation, using a Rigaku AFC-6R diffractometer and rotating anode. Data reduction and refinement were performed with XTAL 3.0.[13] Atomic scattering factors for neutral atoms and real and imaginary dispersion terms were taken from standard sources.[14] For both **I** and **II**, data were collected in two shells, firstly $3° < 2\theta < 80°$ and then $80° < 2\theta < 120°$. Corrections were made for Lorentz and polarization effects, for absorption, and for crystal decay (9% for **I**; 50% overall for **II**). At the point of completion of the inner shell of **II**, the intensities of the standards had decreased by less than 10%. As a consequence, the strong inner reflections, which dominate the refinement of the atomic positions, were not seriously affected by the decay of the crystal. Therefore we are confident that no significant systematic error has been introduced to the metric parameters of **II** from this source. The space groups $P2_1/m$ for **I** and and *Pnma* for **II** were confirmed by successful refinement of the structural models. Initial positional parameters were obtained by heavy-atom and Fourier techniques and were refined by full-matrix least-squares cycles. The rhenium and chlorine atoms making up each complex anion were refined anisotropically, and the quaternary nitrogen atoms likewise. In both structures, all cation carbon atoms were found to be disordered across mirror planes and were refined isotropically with half-occupancies and restraints on distances and angles. Hydrogen atoms were included in the structure-factor calculations at calculated positions. Technical aspects of the crystallography are summarized in Table 1, and Re/Cl/N atomic coordinates for $[Bu_4N][Re_2Cl_9]$ and $[Et_4N]_2[Re_2Cl_9]$ are listed in Tables 2 and 3, respectively.

Spin-restricted SCF−Xα−SW calculations adhered exactly to our previous procedure[3,11] and were performed using the standard codes of Cook and Case.[15] Atomic α values were those of Schwarz,[16] valence-electron weighted averages were used for the inter-sphere and outer-sphere regions. Overlapping atomic sphere radii were set at 89% of the corresponding atomic number radii, in accord with the procedure proposed by Norman.[17] A tangential Watson sphere[18] of charge $z+$ was placed at the outer-sphere radius of the $[Re_2Cl_9]^{z-}$ anion. Spherical harmonics up to $L = 3$, 4, and 5 were used in Cl, Re, and outer spheres, respectively. Transition energies were calculated using the Slater transition-state method,[19] and oscillator strengths were calculated using Noodleman's procedure.[20] Relativistic radial wave functions were used for Re in the calculation of the ground-state electronic structure and transition energies, while nonrelativistic wave functions were used for the calculation of the oscillator strengths.[2]

Table 2. Atomic Coordinates and Isotropic Displacement Parameters (Å^2) for $(Bu_4N)[Re_2Cl_9]$ (**I**)

atom[a]	x/a	y/b	z/c	U_{eq}[b]
Re(1)	0.68829(8)	0.75	0.70499(5)	0.0602(3)
Re(2)	0.71278(10)	0.75	0.90973(6)	0.0789(4)
Cl(1)	0.8564(6)	0.75	0.6389(5)	0.117(3)
Cl(2)	0.5769(4)	0.6064(4)	0.5889(2)	0.107(2)
Cl(3)	0.5026(6)	0.75	0.7652(4)	0.117(3)
Cl(4)	0.8039(4)	0.5997(4)	0.8295(3)	0.097(2)
Cl(5)	0.9082(9)	0.75	1.0506(5)	0.171(5)
Cl(6)	0.6232(6)	0.6059(4)	0.9818(3)	0.138(3)
N(1)	0.507(1)	0.25	0.7504(7)	0.060(5)

[a] See Figure 1, for key to atom labels. [b] $U_{eq} = {}^1/_3[\sum_i\sum_j U_{ij} a_i^* a_j^* \mathbf{a_i}\cdot\mathbf{a_j}]$.

Table 3. Atomic Coordinates and Isotropic Displacement Parameters (Å^2) for $(Et_4N)_2[Re_2Cl_9]$ (**II**)

atom[a]	x/a	y/b	z/c	U_{eq}[b]
Re(1)	0.24305(9)	0.25	0.41582(6)	0.0874(8)
Re(2)	0.2068(1)	0.25	0.30902(6)	0.1072(9)
Cl(1)	0.1473(6)	0.25	0.4937(4)	0.135(6)
Cl(2)	0.3204(4)	0.442(1)	0.4629(3)	0.113(3)
Cl(3)	0.3535(5)	0.25	0.3413(3)	0.094(4)
Cl(4)	0.1597(5)	0.460(1)	0.3734(3)	0.165(5)
Cl(5)	0.0713(7)	0.25	0.2674(5)	0.22(1)
Cl(6)	0.2462(5)	0.449(1)	0.2438(3)	0.133(4)
N(1)	0.520(1)	0.75	0.3501(7)	0.088(8)

[a] See Figure 1, for key to atom labels. [b] $U_{eq} = {}^1/_3[\sum i\sum j U_{ij} a_i^* a_j^* \mathbf{a_i}\cdot\mathbf{a_j}]$.

Results and Discussion

Crystal Structures. Thermal ellipsoid plots and critical dimensions of the two nonahalide anions are shown in Figure 1. In gross terms, $[Re_2Cl_9]^-$ and $[Re_2Cl_9]^{2-}$ are isostructural. Each is revealed as a bioctahedron fused at Cl(1), Cl(2), and Cl(3), with a single mirror plane containing the two crystallographically independent Re atoms together with Cl(3) and the two terminal chloride ligands disposed *trans* to Cl(3). In the case of $[Re_2Cl_9]^{2-}$, this resolves the long-standing question[12] of whether the $(Re^{III}Re^{IV})_2$ state might favor the alternative chloro-capped square-prismatic structure (derived formally by axial Cl^- addition to recently characterized[21] $[Re_2Cl_8]^-$). For $[^nBu_4N][Re_2Cl_9]$, despite the technical difficulties associated with cation disorder (which presumably beset the 1969 determination[9] as well), the accurate geometric data gathered here generally coincide with the less precise dimensions[10] quoted earlier. For example, the values for Re−Re are 2.704(1) and 2.703(13) Å, respectively. Moreover, isomorphous $[^nBu_4N][Re_2Br_9]$ (under refinement in our laboratory) has Re−Re = 2.758-

(12) Bonati. F.; Cotton, F. A. *Inorg. Chem.* **1967**, *6*, 1353.
(13) Hall, S. R., Flack, H. D., Stewart, J. M., Eds. *XTAL3.2 Reference Manual*; Universities of Western Australia, Geneva, and Maryland: Perth, Australia, Geneva, Switzerland, and College Park, MD, 1992.
(14) Cromer, D. T.; Waber, J. T. *International Tables for X-ray Crystallography*; Kynoch Press: Birmingham, England, 1974; Vol. IV.
(15) Cook, M.; Case, D. A. *QCPE* **1982**, *4*, No. 465.
(16) Schwarz, L. *Theor. Chim. Acta* **1974**, *34*, 225.
(17) Norman, J. G. *Mol. Phys.* **1976**, *31*, 1191.
(18) Watson, R. E. *Phys. Rev.* **1958**, *111*, 1108.
(19) Slater, J. C. *Adv. Quantum Chem.* **1972**, *6*, 1.
(20) Noodleman, L. *J. Chem. Phys.* **1976**, *64*, 2343.
(21) Heath, G. A.; Raptis, R. G. *J. Am. Chem. Soc.* **1993**, *115*, 3768

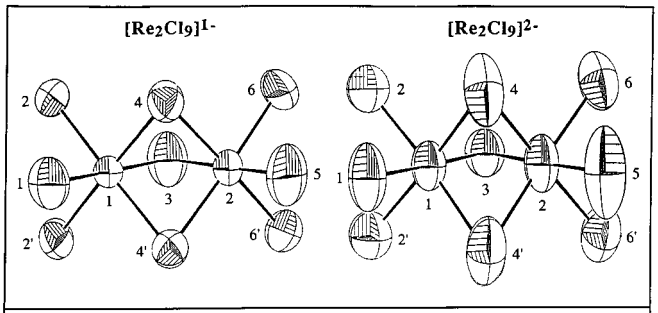

Re(1)-Re(2) / Å	2.704(1)	2.473(4)	Re(1)-Re(2) / Å
Re-Cl_{br} / Å	2.407(4)	2.424(9)	Re-Cl_{br} / Å
Re-Cl_t / Å	2.283(5)	2.322(9)	Re-Cl_t / Å
Re-Cl_{br}-Re / °	68.4(2)	61.3(1)	Re-Cl_{br}-Re / °
Cl_{br}-Re-Cl_{br} / °	91.5(1)	96.3(4)	Cl_{br}-Re-Cl_{br} / °
Cl_t-Re-Cl_t / °	91.4(2)	90.6(3)	Cl_t-Re-Cl_t / °

Figure 1. Thermal ellipsoid plots (50% probability) and comparative structural parameters for $[Re_2Cl_9]^-$ and $[Re_2Cl_9]^{2-}$.

Table 4. Calculated Eigenvalues and Compositions of the Molecular Orbitals of $[Re_2Cl_9]^-$ and $[Re_2Cl_9]^{2-}$ [a]

$[Re_2Cl_9]^-$					$[Re_2Cl_9]^{2-}$				
level	energy/ cm^{-1}	Re	Cl_{br}	Cl_t	level	energy/ cm^{-1}	Re	Cl_{br}	Cl_t
9e′	−34 500	45	18	28	9e′	−29 500	45	19	26
7e″	−39 700	47	16	31	7e″	−32 000	52	12	29
$5a_2''$	−50 900	70	8	16	$5a_2''$	−39 800	68	10	13
6e″	−58 700	66	2	23	6e″	−49 200	70	4	17
8e′	−60 600	58	11	20	8e′	−55 100	59	12	17
$6a_1'$	−67 500	46	9	34	$6a_1'$	−65 700	40	8	42
$2a_2'$	−74 600	0	11	78	$2a_2'$	−68 000	0	12	77
5e″	−74 900	1	11	78	5e″	−68 100	1	12	76
7e′	−75 700	0	9	79	7e′	−69 200	0	10	78
$1a_1''$	−76 000	0	0	88	$1a_1''$	−69 600	0	0	87
$4a_2''$	−77 400	3	36	52	$4a_2''$	−70 500	2	35	53
6e′	−80 100	4	39	46	6e′	−73 100	3	33	53
4e″	−83 300	11	20	57	4e″	−75 700	7	17	62
$1a_2'$	−83 600	0	75	10	$1a_2'$	−78 200	0	75	10
5e′	−85 900	8	31	51	$5a_1'$	−78 800	16	21	55
$5a_1'$	−87 500	9	27	55	5e′	−79 800	8	29	52
$4a_1'$	−89 700	33	2	52	$3a_2''$	−83 200	11	8	67
$3a_2''$	−90 300	14	9	65	$4a_1'$	−84 800	32	12	42
3e″	−91 700	15	23	49	3e″	−85 400	14	19	55
4e′	−95 400	21	39	24	4e′	−88 500	19	40	23
$2a_2''$	−102 600	19	33	39	2e″	−92 000	33	28	35
2e″	−102 700	38	24	38	$2a_2''$	−94 500	18	34	37

[a] The remainder of the electron density (<20% in each case) is located in the inner- and outer-sphere regions of the molecule.

(2) Å, which is a concordant finding for the $(Re^{IV,IV})_2$ internuclear separation given that corresponding $M_2Cl_9^{z-}$ and $M_2Br_9^{z-}$ structures differ typically by 0.05−0.10 Å in their M−M distance.

Comparing $[Re_2Cl_9]^-$ and $[Re_2Cl_9]^{2-}$ (as summarized in Figure 1), one finds both Re−Cl_{br} bond and Re−Cl_t lengths are consistently longer in the reduced species, by about 0.02 and 0.04 Å, respectively. Despite this expansion, there is a marked *decrease* of 0.231(5) Å in the Re−Re separation, associated with the much more acute Re−Cl_{br}−Re angle of 61.3°. To put these dimensions in context, it is interesting to note that in the neighboring complexes, triply-bonded $\{d^3d^3\}$ $[W_2Cl_9]^{3-}$ and frankly nonbonded $\{d^6d^6\}$ $[Ir_2Cl_9]^{3-}$, the internuclear separation changes from 2.41 to 3.15 Å, respectively, with bridgehead angles of 62.4° (W_2) and 85.1° (Ir_2).[7,22]

(22) Gheller, S. F.; Heath, G. A.; Hockless, D. C. R. Manuscript in preparation for publication.

Table 5. Xα-Calculated Transition Energies ($\Delta W/cm^{-1}$), Corrected[a] Transition Energies ($h\nu_{calc}/cm^{-1}$), and Oscillator Strengths (f_{calc}) for $[Re_2Cl_9]^-$ and $[Re_2Cl_9]^{2-}$

transitions	$[Re_2Cl_9]^-$			$[Re_2Cl_9]^{2-}$			class[b]
in D_{3h} sym	ΔW	$h\nu_{calc}$[a]	f_{calc}	ΔW	$h\nu_{calc}$[a]	f_{calc}	$\alpha/\epsilon/\delta/\gamma$
$\sigma \rightarrow \sigma^*$							
$6a_1' \rightarrow 5a_2''$	16 800	26600	0.500	26300	35500	0.446	α_1
XMCT							
5e″ → 6e″	18 000	25 500	0.019	21 200	28 700	0.012	ϵ_1
7e′ → 6e″	18 800	26 300	0.059	22 300	29 800	0.067	ϵ_2
$1a_1'' \rightarrow 6e''$	19 300	26 800	0.045	23 100	30 600	0.035	ϵ_3
$4a_2'' \rightarrow 6e''$	20 500	28 000	0.020	23 400	30 900	0.033	ϵ_4
6e′ → 6e″	23 200	30 700	0.040	25 900	33 400	0.041	ϵ_5
4e″ → 6e″	25 900	33 400	0.001	28 300	35 800	0.004	ϵ_6
5e′ → 6e″	28 700	36 200	0.048	32 400	39 900	0.011	ϵ_7
$3a_2'' \rightarrow 6e''$	32 800	40 300	0.010	35 800	43 300	0.005	ϵ_8
3e″ → 6e″	34 200	41 700	0.001	37 600	45 100	0.015	ϵ_9
5e″ → $5a_2''$	26 100	33 600	0.012	30 600	38 100	0.004	δ_1
4e″ → $5a_2''$	33 900	41 400	0.080	37 700	45 200	0.092	δ_2
5e″ → 7e″	36 200	43 700	0.017	37 500	45 000	0.022	γ_1
7e′ → 7e″	37 000	44 500	0.003	38 600	46 100	0.007	γ_2
$1a_1'' \rightarrow 7e''$	37 500	45 000	0.001	39 400	46 900	0.000	γ_3
$2a_2' \rightarrow 9e'$	41 100	48 600	0.004	39 700	47 200	0.003	γ_4
5e″ → 9e′	41 400	48 900	0.056	39 800	47 300	0.043	γ_5
$4a_2'' \rightarrow 7e''$	38 500	46 000	0.181	39 700	47 200	0.147	γ_6

[a] $h\nu_{calc}$ derived as follows (see text): for $\sigma \rightarrow \sigma^*$ band, from eq 1 with $K = 8000\ cm^{-1}$; for XMCT bands, $h\nu_{calc} = [\Delta W + \delta_{CT}]$ with $\delta_{CT} = 7500\ cm^{-1}$. [b] See Figure 2 for band classifications.

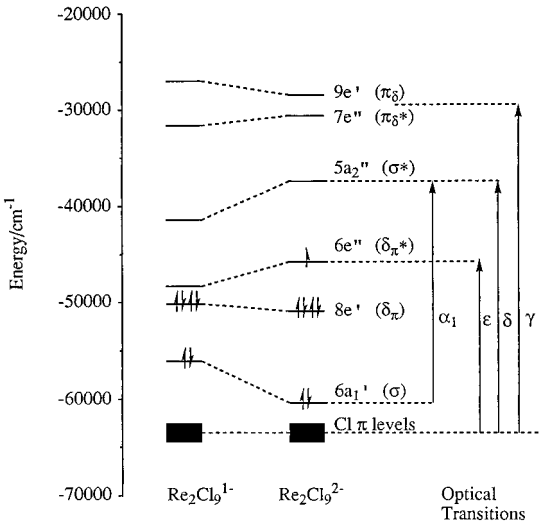

Figure 2. Comparative molecular orbital diagram for $[Re_2Cl_9]^-$ and $[Re_2Cl_9]^{2-}$.

In the present discussion, in order to make faithful comparisons with literature data, we have followed custom and *omitted* geometric thermal-motion corrections. These contribute l% or less to bond lengths in $[Re_2Cl_9]^-$ and $[Re_2Cl_9]^{2-}$ (Tables S5 and S15 Supporting Information), leaving the measured difference in Re−Re essentially unchanged at 0.244(5) Å.

Electronic Structure. The nature of the M_2X_9 molecular orbital diagram has been discussed extensively elsewhere,[1,11] and only the features which bear significantly on the metal−metal interaction are examined here. The calculated eigenvalues and molecular orbital compositions for $[Re_2Cl_9]^-$ and $[Re_2Cl_9]^{2-}$ are compared in Table 4 and presented graphically in Figure 2. In the figure, the calculated levels for $[Re_2Cl_9]^{2-}$ have been lowered uniformly by 6600 cm^{-1} to align the strictly nonbonding chloride-based $2a_2'$ frontier orbital with the corresponding $2a_2'$ level in $[Re_2Cl_9]^-$. (In both systems, $2a_2'$ is virtually isoenergetic with the 5e″ halide donor level which is more prominent in the discussion that follows.) It is legitimate to adopt a point of reference such as this when comparing Xα calculations, since

the computed zero of energy is already made arbitrary by the presence of the Watson sphere and varies from one system to the next. The labels δ_π and π_δ were introduced[3] to emphasise that δ- and π-arrangements transform together under D_{3h} symmetry, so that the 8e′ and 6e″ levels approach $^2/_3\delta$:$^1/_3\pi$ M−M bonding character, while the accompanying 9e′ and 7e″ levels appproach $^2/_3\pi$:$^1/_3\delta$.

The electronic coupling between the metal centers in $[Re_2Cl_9]^-$ has been likened elsewhere[23] to the W−W triple bond of $[W_2Cl_9]^{3-}$, in accord with their shared $(\sigma)^2(\delta_\pi)^4$ ground-state electronic configuration. Cotton has always been more circumspect[1,10] regarding the net bonding in $[Re_2Cl_9]^-$. We can now report that the computed separation between occupied δ_π (8e′) and vacant δ_π* (6e″) components is only 1900 cm^{-1}, and the thermodynamic contribution of the occupied δ_π level to Re−Re bonding is consequently negligible. In contrast, the computed $\sigma-\sigma$* separation is approximately 17 000 cm^{-1}, much as it is[3] in $\{d^5d^5\}$ $[Os_2X_9]^{3-}$. Therefore, *from a structural and energetic perspective*, it is much more realistic to regard the $Re^{IV}-Re^{IV}$ bond as effectively single in nature. The observed metal−metal distance (2.704 Å) is consistent with this view. In this respect the $[Re_2Cl_9]^-$ anion resembles diagonally related, isoelectronic $[Mo_2Cl_9]^{3-}$ whose electronic structure has been recently discussed in detail by Stranger and co-workers.[24] In the second-row $\{d^3d^3\}$ complex, the σ electrons are found to be strongly coupled but the four electrons in the δ_π level are essentially noninteracting and make no significant contribution to metal−metal bonding. The relative unimportance of the δ_π component has been advanced as a possible explanation for the marked lattice dependence of the Mo−Mo bond length, which varies from 2.52 to 2.82 Å in different salts.[24] In both $[Re_2Cl_9]^-$ and $[Mo_2Cl_9]^{3-}$, we believe that the description of the metal−metal interaction as a triple bond, in accord with the formal bond order, is naive. In particular, the crucial distinction between the σ and δ_π components of the bond, which have very different structural and energetic consequences, is obscured.

Returning to the present crystallographic comparison of $[Re_2Cl_9]^-$ and $[Re_2Cl_9]^{2-}$, Figure 1 reveals that the Re−Re bond shortens substantially upon one-electron reduction, despite the slight extension of the $Re-Cl_{br}$ bonds. This is a striking observation, because the additional electron enters a Re−Re antibonding δ_π* orbital, thereby *lowering* the formal bond order from 3 to 2.5. However, the nominal change in bond order is only one of several factors to be considered. Upon one-electron reduction, the net positive charge on each metal center is lowered, resulting in a diminished electrostatic repulsion between the two rhenium ions. In addition, the single-ion 5d "t_{2g}" orbitals expand radially in the lower oxidation state, resulting in more effective overlap between the neighboring metal centers. Figure 2 indicates that the $\sigma-\sigma$* separation approaches 27 000 cm^{-1} in the dianion, an increase of over 50%. Moreover, in $[Re_2Cl_9]^{2-}$ the computed $\delta_\pi-\delta_\pi$* gap is 7000 cm^{-1}, more than three times greater than in $[Re_2Cl_9]^-$, suggesting the emergence of a significant δ_π component to the Re−Re bonding upon reduction.

The substantially shorter metal−metal separation in $(\sigma)^2(\delta_\pi)^4(\delta_\pi^*)^1$ $[Re_2Cl_9]^{2-}$ implies that these factors (diminished electrostatic repulsion, stronger σ-bond, δ-bonding "switched on") combine synergically to enhance the Re−Re interaction in the reduced species and that they outweigh the destabilizing effect of populating the weakly antibonding δ_π* orbital. A similar phenomenon is observed for the $[Tc_2Cl_8]^{2-/3-}$ couple,[25,26] where a marginal decrease (0.03 Å) in Tc−Tc bond length occurs upon reduction, despite the loss of half a δ bond. The $[Re_2Cl_9]^{1-/2-}$ system clearly provides a much more dramatic demonstration of the valence-linked stabilizing influence of orbital expansion and diminished electrostatic repulsion. The importance of purely electrostatic effects is shown by the molecular geometry of the instructive closed-shell archetype, $[Ir_2Cl_9]^{3-}$. In this rigorously nonbonding situation, the measured $M^{3+}-M^{3+}$ separation[22] of 3.15 Å is *0.47 Å greater* than it would be if the complex anion retained the 70.25° bridgehead angle of the naive "ideal bioctahedron".

Optical Spectra. Earlier accounts of the electronic spectra of $[Re_2Cl_9]^-$ and $[Re_2Cl_9]^{2-}$,[12,23] and of electrogenerated $[Re_2Cl_9]^{3-}$,[6] made no attempt to provide explicit assignments within a molecular orbital description or to locate the crucial $\sigma-\sigma$* transition. However, a consistent theoretical analysis of the spectra of the $\{d^5d^5\}$ bimetallic nonahalides $[Ru_2X_9]^{3-}$ and $[Os_2X_9]^{3-}$ (X = Cl, Br) has recently emerged,[3,11] and we are now in a position to extend that study to encompass the rhenium system. The low-temperature, linear-frequency electronic spectra of $[Re_2Cl_9]^{z-}$ ($z = 1-3$) from ref 6 are reproduced in Figure 3.

As a general rule, the intense halide-to-metal charge-transfer (XMCT) envelopes of isostructural $4d^n$ and $5d^n$ transition metal complexes are notably similar in appearance, but their position varies dramatically throughout the near-IR to far-UV spectrum, according to the identity of X and M. The three salient principles emerging from our earlier work[3,11] may be summarized as follows. Firstly, an experimental and computational survey of several MX_6 and M_2X_9 complexes has demonstrated that the calculated XMCT transition energies are *faithfully linearly related* to the observed bands, even though the latter are widely distributed between 12 000 and 48 000 cm^{-1}. Throughout this range, the calculated energies are deficient by 7000−8000 cm^{-1}, but uniformly so. The physical basis of this error in the Xα description is well-understood in qualitative terms,[27] but its crucial constancy in simple halide complexes had not been recognized. This discovery means that it is proper to add a fixed correction factor, δ_{CT}, of 7500 cm^{-1} to the computed XMCT transition energies for the purposes of predicting or recognizing the experimental bands. Secondly, computed oscillator strengths appear to reliably model relative XMCT band intensities, and taken collectively, they are a considerable aid to assignment. For example, the anticipated low-lying Xπ to σ* excitation ($5e'' \rightarrow 5a_2''$) turns out to be specifically unfavored, and of negligible intensity, in the trigonal M_2X_9 systems. Thirdly, within the metal−metal manifold, an energetic correction of a different nature is required for those excitations which have the net effect of uncoupling electron pairs. In $[Ru_2X_9]^{3-}$, for example, the metal-centered $\sigma \rightarrow \sigma$* transition is observed approximately 10 000 cm^{-1} above the calculated separation between σ and σ* orbitals,[11] as a consequence of the neglect of electron correlation in the SCF−Xα−SW wave function. The relationship between observed and computed transition energies for the $(\sigma)^2(\sigma^*)^0 \rightarrow (\sigma)^1(\sigma^*)^1$ process can be generalized as shown.[28]

(23) Strubinger, S. K. D.; Sun, I. W.; Cleland, W. E., Jr.; Hussey, C. L. *Inorg. Chem.* **1990**, *29*, 4246.
(24) Stranger, R.; Moran, G.; Krausz, E.; Medley, G. *Inorg. Chem.* **1993**, *32*, 4555.
(25) Cotton, F. A.; Daniels, L.; Davison, A.; Orvig, C. *Inorg. Chem.* **1981**, *20*, 3051.
(26) Cotton, F. A.; Shive, L. W. *Inorg. Chem.* **1975**, *14*, 2032.
(27) Case, D. A.; Aizmann, A. *Inorg. Chem.* **1981**, *20*, 528. Desjardins, S. R.; Penfield, K. W.; Cohen, S. L.; Musselman, R. L.; Solomon, E. I. *J. Am. Chem. Soc.* **1983**, *105*, 4590.
(28) Hopkins, M. D.; Gray, H. B.; Miskowski, V. M. *Polyhedron* **1987**, *6*, 705.

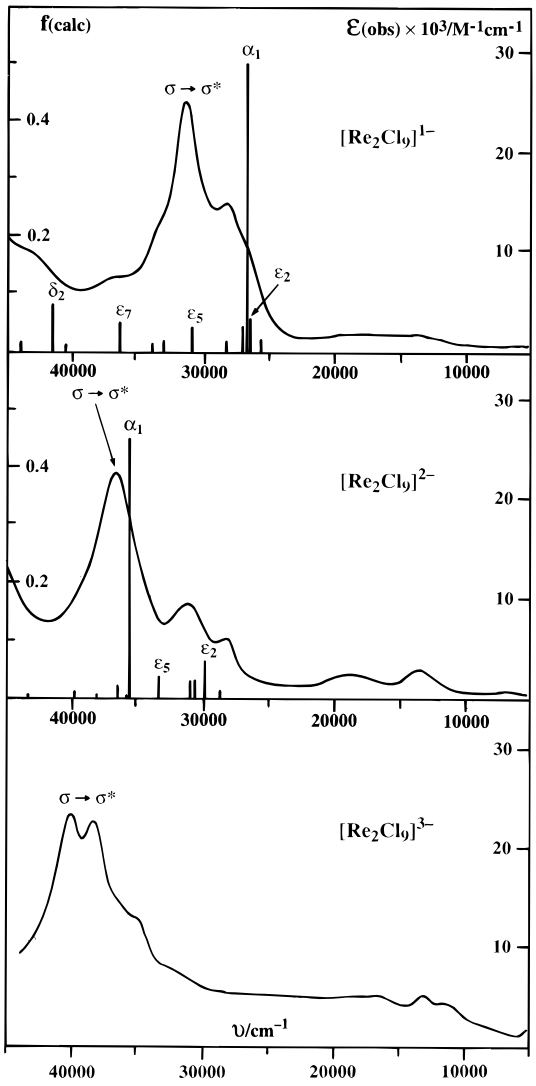

Figure 3. Optical spectra of $[Re_2Cl_9]^-$, $[Re_2Cl_9]^{2-}$, and $[Re_2Cl_9]^{3-}$ in CH_2Cl_2 at 190 K, showing the suggested progression in the $\sigma \rightarrow \sigma^*$ bond. Calculated transitions from Table 5 are inscribed.

$$h\nu = (K^2 + \Delta W^2)^{1/2} + K \qquad (1)$$

Here, $h\nu$ is the (predicted) location of the observed band, ΔW is the uncorrected transition energy (derived[19] from the Xα-computed energy separation between σ and σ^* orbitals), and K is the appropriate electron-exchange term which is typically[3,11] of the order of 8000 cm^{-1}. In the present context it is important to note that the *z*-polarised $\sigma \rightarrow \sigma^*$ promotion retains the same essential $(\sigma)^2(\sigma^*)^0 \rightarrow (\sigma)^1(\sigma^*)^1$ nature, and presumably much the same electron-correlation term, whatever the occupancy (0, 1, or 2) of the uninvolved δ_π^* level. That is, we should be able to track this particular transition in a regular way through the series $[Re_2Cl_9]^-$, $[Re_2Cl_9]^{2-}$, and $[Re_2Cl_9]^{3-}$.

Calculated transition energies and oscillator strengths for significant dipole-allowed transitions of $[Re_2Cl_9]^-$ and $[Re_2Cl_9]^{2-}$ are summarized in Table 4. Promotions within the metal−metal manifold are denoted α, while CT promotions to 6e″, to $5a_2''$, and to {7e″, 9e′} are denoted ϵ, δ, and γ, respectively. The $\sigma \rightarrow \sigma^*$ transition ($6a_1' \rightarrow 5a_2''$) is α_1. The more important transitions are inscribed schematically in Figure 3, where the theoretical CT energies have already been augmented by δ_{CT} (7500 cm^{-1}), and $\sigma \rightarrow \sigma^*$ has been corrected for electron correlation as specified in Table 4. Transitions formally related to the single-ion ligand-field transition (in that they interconnect levels derived from the t_{2g} and e_g orbitals of the parent octahedron) are not included in the table, as all have calculated oscillator strengths less than 0.02.

In the first instance, the main features are most readily assigned in the spectrum of odd-electron $\{d^5d^6\}$ $[Re_2Cl_9]^{2-}$. The moderately intense bands in the region of 30 000 cm^{-1} are attributable to a series of Cl → 6e″ CT transitions ($\epsilon_{2,3,4}$). However, on the grounds of both position and intensity, the dominant feature at 36 400 cm^{-1} cannot be persuasively accounted for by the ϵ series. The lowest energy Cl → $5a_2''$ transition (δ_1) lies in the appropriate energy range, but as noted above,[11] this transition tends to have negligible intensity, especially for $[Re_2Cl_9]^{2-}$. The high-oscillator-strength γ_5 and γ_6 transitions, which were prominent in the ultraviolet region of the spectra of the $\{d^5d^5\}$ Ru_2 and Os_2 systems,[3,11] are reliably predicted to lie above 45 000 cm^{-1} for both $[Re_2Cl_9]^-$ and $[Re_2Cl_9]^{2-}$ (after inclusion of δ_{CT}) and will be further blue-shifted upon reduction to $[Re_2Cl_9]^{3-}$. In other words, γ_5 and γ_6 are too energetic to fall within the recorded spectra of the $[Re_2Cl_9]^{z-}$ series. The only other eligible transition is the *z*-polarized $\sigma \rightarrow \sigma^*$ excitation. This is predicted by eq 1 to lie at 35 500 cm^{-1}, in remarkable accord with the observed band maximum.

Interpretation of the spectrum of $[Re_2Cl_9]^-$ is somewhat more challenging, because the CT and $\sigma \rightarrow \sigma^*$ transitions are now calculated to overlap. (Even intuitively, both band types would be expected to be red-shifted with respect to their position in $[Re_2Cl_9]^{2-}$, so one cannot differentiate between them on this qualitative basis.) Visual comparison of the whole series suggests that the dominant feature at 31 000 cm^{-1} for $[Re_2Cl_9]^-$, resembling the intense band in $[Re_2Cl_9]^{2-}$, is due to the $\sigma \rightarrow \sigma^*$ transition, while the shoulder at lower energy should be assigned once again to the Cl → 6e″ CT manifold. An alternative assignment, attributing the shoulder to the $\sigma \rightarrow \sigma^*$ transition, offers a closer match with the calculated transition energy (corrected as above for electron correlation), however, this choice would leave no obvious explanation for the much greater intensity of the peak at 31 000 cm^{-1}.

Given the marked success of the model in predicting the band position in $[Re_2Cl_9]^{2-}$ and in the $\{d^5d^5\}$ systems described earlier, the apparent discrepancy between observed and calculated $\sigma \rightarrow \sigma^*$ transition energies in $[Re_2Cl_9]^-$ is worth further consideration. It may of course reflect limitations inherent in the model, such as use of a constant value for the exchange integral, *K*. Alternatively, the relatively high frequency of the observed absorption band may signify that the Re−Re separation for $[Re_2Cl_9]^-$ in solution is actually somewhat smaller than the crystallographic value employed in the calculation. The similarities in electronic structure of the $[Re_2Cl_9]^-$ and $[Mo_2Cl_9]^{3-}$ anions, and the tendency for the Mo−Mo separation to vary widely among different salts,[24] have been noted above.

It remains to extend the above analysis to the spectrum of the Re^{III}_2 anion, $[Re_2Cl_9]^{3-}$. This doubly-reduced species is prone to rapid dissociation to form familiar $[Re_2Cl_8]^{2-}$ [23] but has been characterized by *in situ* spectroelectrochemistry[6] at very low temperature. In CH_2Cl_2 solution at 188 K, electrochemical interconversion of $[Re_2Cl_9]^{2-}$ and $[Re_2Cl_9]^{3-}$ is fully reversible, consistent with (though not proving) our belief that the triply-halide-bridged structure is retained in the latter. The pattern of electrode potentials[6] and the optical spectrum both support this view. Thus, the UV absorption envelope of $[Re_2Cl_9]^{3-}$ is quite distinct from that of isovalent $[Re_2Cl_8]^{2-}$ but bears a family resemblance to that of $[W_2Cl_9]^{3-}$. The spectrum of $[Re_2Cl_9]^{3-}$ reveals a further shift of the intense manifold, with twin maxima at 38 200 and 40 100 cm^{-1}

compared to the maxima at 36 400 cm^{-1} for $[Re_2Cl_9]^{2-}$ and 30 900 cm^{-1} for $[Re_2Cl_9]^{-}$.

This trend suggests in turn that, upon addition of a second electron, the Re−Re interaction is further enhanced relative to the dianion, despite the reduction in formal bond order to 2.0. It appears that the stabilizing effects of reduced cation−cation repulsion and of expansion of the metal d orbitals continue to outweigh the antibonding influence of each newly added δ_π* electron. Structural information on highly reactive $[Re_2Cl_9]^{3-}$ is unlikely to arise from conventional crystallographic analysis, so the extent to which the blue shift of the $\sigma \rightarrow \sigma$* band reflects a further contraction in the Re−Re bond length is a matter of conjecture. We note the observed metal−metal separation in the dianion, $[Re_2Cl_9]^{2-}$, is already close to that in triply bonded $[W_2Cl_9]^{3-}$ (2.42 Å),[8] which represents the closest approach of two M^{III} ions within the series of nonachlorides. Consequently a further marked contraction of the Re−Re separation upon reduction to $[Re_2Cl_9]^{3-}$ seems unlikely. However, even at constant metal−metal separation, orbital dilation in the trianion will result in enhanced $\sigma-\sigma$* and $\delta_\pi-\delta_\pi$* separations. It may be that this enhanced σ and δ_π bonding figures intimately in the collapse of the bridging architecture and the adoption of face-to-face geometry in the formation of $[Re_2Cl_8]^{2-}$, where the four electrons in π and δ levels contribute maximally to multiple bonding, and the Re−Re separation is only 2.24 Å.

Conclusions

The molecular structures of the two complex ions, $[Re_2Cl_9]^{-}$ and $[Re_2Cl_9]^{2-}$, determined by X-ray diffraction, indicate that the Re−Re interaction is much stronger in the dianion, despite a reduction in formal bond order from 3.0 to 2.5. Quantitative calculations of the electronic structure show that the δ_π component of the bonding is negligible at the $(Re^{IV})_2$ level. Therefore, the metal−metal interaction in $[Re_2Cl_9]^{-}$ should be logically and realistically regarded as a single Re−Re bond notwithstanding the $\{d^3d^3\}$ configuration. This conclusion illustrates once again the limited utility of the ordinal concept of bond order in rationalizing structural trends. The $\{d^3d^3\}$ configuration, and hence the formal bond order of 3, encompasses a continuum of actual bonding situations, ranging from weak coupling of all electrons ($[Cr_2Cl_9]^{3-}$), through to strong metal−metal bonding ($[W_2Cl_9]^{3-}$). The situation in $[Re_2Cl_9]^{-}$ is intermediate between these extremes, with the σ electrons forming a strong single bond, but the four remaining δ_π electrons make a negligible contribution to the overall Re−Re bond strength.

In $[Re_2Cl_9]^{2-}$, with a measured Re−Re distance of only 2.47 Å, the σ component of the Re−Re bond is considerably strengthened relative to $[Re_2Cl_9]^{-}$, and in addition a significant δ_π component to the bond also develops. The enhanced bonding is ascribed jointly to diminished cation−cation repulsion within the MX_3M core (which contributes materially to the smaller Re−Re separation) and to radial expansion of the single-ion t_{2g} orbitals in the reduced species.

The electronic spectra of structurally characterized $[Re_2Cl_9]^{-}$ and $[Re_2Cl_9]^{2-}$ have a ready explanation within the theoretical framework developed previously,[11] and this analysis leads us to propose that in both systems the dominant ultraviolet absorption band corresponds to the $\sigma \rightarrow \sigma$* transition. This also apppears to hold for the fully reduced $(Re^{III})_2$ complex, $[Re_2Cl_9]^{3-}$, in which case the spectrum provides evidence for further enhancement of the Re−Re σ interaction upon addition of the second electron. In any event, a picture emerges of both XMCT and $\sigma \rightarrow \sigma$* transitions contributing to the intense absorption envelope which shifts consistently to higher frequency across the series $[Re_2Cl_9]^{-}$, $[Re_2Cl_9]^{2-}$, and $[Re_2Cl_9]^{3-}$. We also note that δ_π bonding in $[Re_2Cl_9]^{3-}$, while thermodynamically favorable in itself, may yet play an intimate mechanistic role in directing the rearrangement to isovalent $[Re_2Cl_8]^{2-}$.

Considered more broadly, the present study has allowed us to reconcile the available structural, electrochemical, optical, and computational evidence in arriving at a satisfactory account of bonding in $[Re_2Cl_9]^{z-}$ ($z = 1-3$), and it illustrates the benefits of considering such data in a wider descriptive context of neighboring binuclear systems. To return to our opening theme, the wealth of isostructural transition-metal M_2X_9 complexes provides an excellent basis for systematic study of periodic progressions in metal−metal bonding. These progressions are increasingly revealed as an elegant, interdependent function of $4d^n$ or $5d^n$ configuration, oxidation state, and underlying core charge or atomic number.

Acknowledgment. This work was supported by the Institute of Advanced Studies (ANU) and by provision of an SERC (U.K.) overseas studentship (to J.E.M.).

Supporting Information Available: Text giving details of refinement of **I** and **II** and Tables S1−S9 and S10−S18 listing atomic coordinates (including those for Bu_4N^+ and Et_4N^+), anisotropic displacement parameters, interatomic distances, interatomic angles, torsion angles, least-squares planes, and nonbonded contacts (36 pages). Ordering information is given on any current masthead page.

IC951604K